

Prior Knowledge Uses Prestimulus Alpha Band Oscillations and Persistent Poststimulus Neural Templates for Conscious Perception

 Lu Shen,^{1,2*} Zehua Wu,^{3*} Zhenzhu Yue,³ Bing Li,⁴ Qi Chen,^{1,2} and Biao Han^{1,2}

¹Center for Studies of Psychological Application, South China Normal University, Guangzhou 510631, China, ²School of Psychology, South China Normal University, Guangzhou 510631, China, ³Department of Psychology, Guangdong Provincial Key Laboratory of Social Cognitive Neuroscience and Mental Health, Sun Yat-sen University, Guangzhou 510275, China, and ⁴Department of Psychology, Jilin University, Changchun 130012, China

Prior knowledge has a profound impact on the way we perceive the world. However, it remains unclear how the prior knowledge is maintained in our brains and thereby influences the subsequent conscious perception. The Dalmatian dog illusion is a perfect tool to study prior knowledge, where the picture is initially perceived as noise. Once the prior knowledge was introduced, a Dalmatian dog could be consciously seen, and the picture immediately became meaningful. Using pictures with hidden objects as standard stimuli and similar pictures without hidden objects as deviant stimuli, we investigated the neural representation of prior knowledge and its impact on conscious perception in an oddball paradigm using electroencephalogram (EEG) in both male and female human subjects. We found that the neural patterns between the prestimulus alpha band oscillations and poststimulus EEG activity were significantly more similar for the standard stimuli than for the deviant stimuli after prior knowledge was provided. Furthermore, decoding analysis revealed that persistent neural templates were evoked after the introduction of prior knowledge, similar to that evoked in the early stages of visual processing. In conclusion, the current study suggests that prior knowledge uses alpha band oscillations in a multivariate manner in the prestimulus period and induces specific persistent neural templates in the poststimulus period, enabling the conscious perception of the hidden objects.

Key words: alpha oscillations; conscious perception; Dalmatian dog illusion; persistent neural templates; prior knowledge

Significance Statement

The visual world we live in is not always optimal. In dark or noisy environments, prior knowledge can help us interpret imperfect sensory signals and enable us to consciously perceive hidden objects. However, we still know very little about how prior knowledge works at the neural level. Using the Dalmatian dog illusion and multivariate methods, we found that prior knowledge uses prestimulus alpha band oscillations to carry information about the hidden object and exerts a persistent influence in the poststimulus period by inducing specific neural templates. Our findings provide a window into the neural underpinnings of prior knowledge and offer new insights into the role of alpha band oscillations and neural templates associated with conscious perception.

Received Feb. 12, 2023; revised July 21, 2023; accepted July 26, 2023.

Author contributions: L.S. and B.H. designed research; L.S., Z.W., and B.H. performed research; L.S., Z.W., Z.Y., B.L., Q.C., and B.H. contributed unpublished reagents/analytic tools; L.S., Z.W., and B.H. analyzed data; and L.S., Z.W., and B.H. wrote the paper.

This work was supported by National Natural Science Foundation of China Grants 32000741 and 32000785; Natural Science Foundation of Guangdong Province Grants 2021A1515011100, 2020A1515110223, and 2021A1515011185; Guangzhou Fundamental Research Program Grants 202102020761 and 202102020274; and Ministry of Education Project of Key Research Institute of Humanities and Social Sciences in Universities Grant 22JJD190006.

*L.S. and Z.W. contributed equally to this work.

The authors declare no competing financial interests.

Correspondence should be addressed to Biao Han at biao.han@m.scnu.edu.cn or Qi Chen at qi.chen27@gmail.com.

<https://doi.org/10.1523/JNEUROSCI.0263-23.2023>

Copyright © 2023 the authors

Introduction

Conscious perception is not solely determined by sensory input. Starting with Helmholtz (1867), perception has been conceptualized as an inference process in which top-down prior knowledge is combined with bottom-up sensory input to construct posterior beliefs that enter our awareness. Especially in the presence of noisy or ambiguous sensory input, prior knowledge guides us in interpreting the imperfect perceptual information and helps us to consciously identify objects and people (Bar, 2004; de Lange et al., 2018). Despite the profound impact of prior knowledge, it remains largely unknown how prior knowledge is maintained in our brains and persistently contributes to our conscious perception.

Previous studies have shown that prior knowledge such as the identity (Mayer et al., 2016; Samaha et al., 2018), location (Samaha et al., 2016), onset time (Samaha et al., 2015; Wilsch et al., 2015), and task demands (Wutz et al., 2018; Han et al., 2023) of an upcoming stimulus is closely related to variations in the prestimulus alpha band oscillations in human studies. *In vivo* recordings from cats and macaques also show that the expectancy of visual stimuli is accompanied by an increase in the power and the interareal interaction of the alpha band (Chatila et al., 1992; L. Mo et al., 2011; von Stein et al., 2000). The existing evidence suggests that alpha band oscillations are viable neural markers for prior knowledge in the brain; however, whether alpha band oscillations actually carry information about prior knowledge remains unknown. On the other hand, previous studies have shown that conscious perception of stimuli is associated with late-onset (>200 ms), long-lasting (~1 s), and more stable neural activity in a variety of brain areas (Li et al., 2014; Schurger et al., 2015) and with stronger neural representations (Salti et al., 2015; King et al., 2016). It remains unclear whether and how prior knowledge modulates the neural representation of the stimuli to enable conscious perception.

The Dalmatian dog illusion is one of the most compelling demonstrations of the dramatic effects of prior knowledge (Gregory, 1970). When the picture was first viewed, it was perceived as a noisy set of meaningless black and gray patches that were difficult to categorize; however, after a simple instruction about the hidden Dalmatian, the dog could be consciously seen, and the subjective perception of the picture immediately became clear and meaningful (van Tonder and Ejima, 2000; Chang et al., 2016; Sadil et al., 2019). There is no doubt that the prior knowledge about the hidden objects plays an important role in our ability to consciously perceive the dog, making such pictures a perfect tool for studying the influence of prior knowledge on conscious perception.

Using the hidden Dalmatian picture and another similar picture with a hidden face (Ahissar and Hochstein, 2004; Albright, 2012), we investigated the retention of prior knowledge and its effect on conscious perception. To establish a minimal contrast (Dehaene, 2014) between consciously seen and unseen stimuli, we constructed nearly identical pictures with and without the hidden object (Fig. 1A). These stimuli were then presented in a task-irrelevant oddball paradigm and assigned as the standard and deviant stimuli, respectively. Initially, both stimuli were perceived as noise, and their subjective perception was similar. However, immediately after the revelation of the hidden object, the previously hidden information becomes consciously accessible. Participants can now consciously perceive and differentiate between the standard and deviant stimuli based on the newly acquired prior knowledge. By using the task-irrelevant oddball paradigm and examining the visual mismatch response, we were able to assess the successful manipulation of prior knowledge and investigate its impact on conscious perception while maintaining experimental control over attentional effects. Our findings, obtained using multivariate methods, demonstrated that prior knowledge uses alpha band neural oscillations to convey information about the hidden objects before stimulus onset. Furthermore, after stimulus onset, prior knowledge induced a persistent neural template associated with the hidden object, facilitating sustained conscious perception.

Materials and Methods

Participants. Twenty-four healthy human participants of either sex participated in the experiment. Two participants were excluded from the

analysis because of excessive noise and artifacts in the EEG data. Analyses were performed on the remaining 22 participants (12 females, 19–25 years old, all right-handed). All participants had normal or corrected-to-normal vision and no history of neurologic or mental illness. None of the participants had been exposed to the experimental materials before this experiment. All participants gave informed consent before the experiment in accordance with the Declaration of Helsinki, and the study was approved by the Ethics Committee of the School of Psychology, South China Normal University.

Stimuli. Two sets of visual stimuli were created by modifying the hidden Dalmatian dog and face pictures (Gregory, 1970; Ahissar and Hochstein, 2004); one set of pictures contains the features of a dog or a human face, and the other set is obtained by flipping the previous set of pictures vertically and does not contain the corresponding features. We then assigned the pictures with and without face or dog features as standard and deviant stimuli, respectively. In this way, we not only minimized the difference in physical properties between the standard and deviant stimuli but also ensured that it was difficult to distinguish between the standard and deviant stimuli in the absence of explicit instructions; however, it was clear in the presence of explicit instructions that the standard stimuli contained a face or a dog, whereas the deviant stimuli did not. For the standard stimuli, the hidden face or dog was embedded in the peripheral upper visual field (~1.5–2° visual angle away from the central fixation point).

To maintain participants' attention on the center fixation point (L. Mo et al., 2011), regardless of whether the stimuli were standard or deviant, a solid or hollow blue square (0.5° × 0.5° visual angle) was presented in the center of the stimuli, identified as the target or nontarget stimulus, respectively.

Experimental design. The experiment consisted of two sessions, the preinstruction session and the postinstruction session. In each session, two blocks containing the dog and two blocks containing the face were presented alternately. The order of the blocks was counterbalanced across participants. Each block contained 200 trials, consisting of 70% standard stimulus trials, 20% deviant stimulus trials, and 10% target stimulus trials. Within each trial, a central fixation point (0.05° × 0.05° visual angle) was first presented for 750 ms, then the stimuli were presented on a gray background for 250 ms. Participants were asked to respond to the target stimuli by pressing a key on the keyboard within 750 ms of stimulus onset (Fig. 1B), regardless of the content of the presented images. If the response was incorrect or missed, a feedback tone was emitted. Target trials and trials with false alarms were excluded from the EEG data analysis.

At the end of the preinstruction session, each participant was given verbal instructions and a picture with cues to reveal either the hidden dog or the hidden face, but not both. Stimuli were further categorized as instructed and noninstructed depending on which picture provided information about the hidden feature. The type of instructed stimuli was counterbalanced across participants (i.e., half of the participants were instructed to detect the face stimulus, and the other half were instructed to detect the dog stimulus). Participants were allowed to continue the experiment until they could clearly report the face or dog in the stimuli and correctly indicate the location of its components (e.g., eye location in the face stimuli, dog head location in the dog stimuli) so that participants could easily perceive a dog or human face in the standard stimuli in the postinstruction session. Participants were asked to complete the postinstruction session with four stimulus blocks containing exactly the same physical stimuli (Fig. 1C). The experiment had an average duration of ~1 h.

In summary, participants were exposed to two conditions in two sessions, the instructed condition and the noninstructed condition in the preinstruction and postinstruction sessions. Each condition contained three different types of trials, standard, deviation, and target stimulus. Stimuli were presented at a distance of 57 cm using a desktop computer with an LCD monitor (resolution, 800 × 600 pixels; refresh rate, 120 Hz). Stimuli were presented using the Psychtoolbox (Brainard, 1997) running in MATLAB (MathWorks), and electroencephalograms (EEGs) were recorded throughout the experiment.

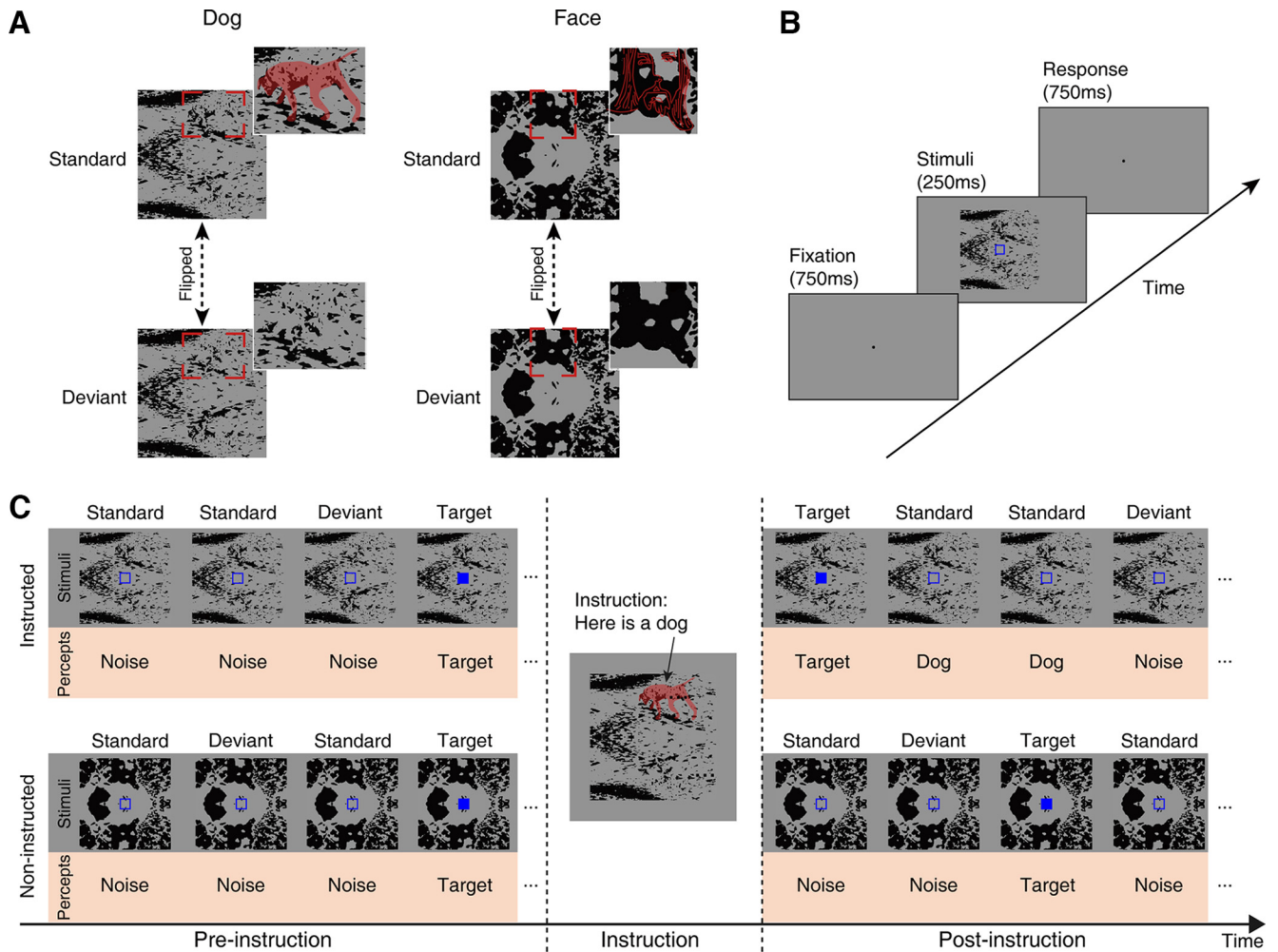


Figure 1. The stimuli and the experimental design. **A**, Two sets of standard and deviant visual stimuli were created by modifying the hidden Dalmatian dog and face pictures. For the standard stimuli, without explicit instructions, the pictures appeared as a set of meaningless black and gray patches that were difficult to categorize. However, when explicit instructions were given, the picture became clear and meaningful and could be easily categorized as a human face or a dog. The deviant stimuli were obtained by flipping the standard stimuli upside down. For the deviant stimuli, as they do not contain information about the hidden Dalmatian dog and face, the pictures remained meaningless even with explicit instructions. The hidden dog and face are colored in red in the magnified pictures. **B**, Time course of a single trial. Regardless of a standard or deviant stimulus, a hollow or solid blue square was always presented in the center of the stimulus, identified as a nontarget or target stimulus, respectively. Participants were instructed to respond only to the target stimuli. The experiment consisted of 70% standard stimulus trials, 20% deviant stimulus trials, and 10% target stimulus trials. **C**, Time course of the whole experiment. The experiment consisted of a preinstruction, postinstruction, and instruction session in between. In the preinstruction session, both the instructed and noninstructed pictures were considered as a set of meaningless black and gray patches of noise. Participants then received information about either the hidden dog or the hidden face during the instruction so that the hidden object would consciously be seen for the instructed picture in the postinstruction session.

EEG acquisition and preprocessing. EEG data were recorded using caps with 62 Ag/Ag-Cl electrodes (10–20 system) with NeuroScan SynAmp Amplifiers (sampling rate, 1000 Hz). The impedance of all electrodes was below 5 k Ω during the recording. The vertical eye movements were recorded by electrodes placed above and below the left eye, and the horizontal eye movements were recorded by electrodes placed on the outer canthi of both eyes. All off-line analyses were performed using FieldTrip software (Oostenveld et al., 2011) and custom scripts in MATLAB. For the off-line preprocessing, the data were downsampled to 256 Hz and converted to an average reference. Then, the continuous EEG data were epoched from –1500 ms before to 2000 ms after stimulus onset. The epoched data were visually inspected, epochs with visual and muscle artifacts were discarded, and noisy electrodes were spherically interpolated. After artifact rejection, ~90% trials were retained. In both the instructed and noninstructed conditions during the preinstruction and postinstruction sessions, we retained ~250 standard trials and 70 deviant trials each. No filtering, including high-pass, low-pass, or notch filters, was applied during the EEG analysis. To perform the subsequent global field power (GFP) and decoding analysis, EEG signals were baseline-corrected at the trial level using a 500–0 ms interval before the stimulus onset for each individual trial.

GFP analysis. GFP is calculated as the SD of the response across channels at each time point (Lehmann and Skrandies, 1980), which is independent of the bias caused by manual selection of electrodes of interest and provides a reliable and direct measure of the total brain activity. GFP at time t is defined as follows:

$$\text{GFP}_t = \sqrt{\frac{1}{n} \sum_{i=1}^n (u_{i,t} - \bar{u}_t)^2},$$

where $u_{i,t}$ is the neural activity for channel i at time t , \bar{u}_t is the mean activity over all channels at time t , and n is the number of channels. GFP computations were performed for standard and deviant trials, respectively. To avoid the confound introduced by the difference in the number of trials, we matched the number of trials for the standard and deviant trials by randomly extracting the number of deviant trials from the standard trials (~70 standard trials and ~70 deviant trials were retained for each condition).

Topographical correlation analysis. We conducted a topographical correlation analysis to assess the neural representational similarity between the prestimulus oscillatory power and the poststimulus EEG

activity. The prestimulus power P_i^f for channel i and frequency f was obtained through a fast Fourier transform (FFT) from -500 to 0 ms relative to the stimulus onset. A zero padding of length $nfft = 256$ was used to improve the frequency resolution of the Fourier transform. To obtain the poststimulus EEG activity, an overlapping sliding window of 100 ms (step size, 3.9 ms) centered on the time point t was first applied to improve the signal-to-noise ratio. Consequently, the EEG activity within the 0 – 50 ms range contained signals originating from the prestimulus window and thus was excluded from the analysis of the poststimulus data. The EEG activity $\hat{u}_{i,t}$ was defined as the square of the mean neural activity for all trials for one condition over the sliding window for the time t and channel i . No baseline correction was applied during the computation of prestimulus power and EEG activity. We quantified the representational similarity between the prestimulus power and the EEG activity using a Spearman correlation across channels as follows:

$$\text{rho}_{i,f} = 1 - \frac{6 \sum_{i=1}^n \left(R(\hat{u}_{i,t}) - R(P_i^f) \right)^2}{n(n^2 - 1)},$$

where n is the total number of channels and $R(x)$ is the rank of the x variable. For further statistical analysis, correlation values were Fisher z transformed.

To eliminate the influence of spontaneous correlations between prestimulus power and poststimulus EEG activity, we used a two-step procedure. First, we calculated the spontaneous correlations, which can naturally arise without any external stimulus, by computing Fisher z transformed and averaged correlation values for prestimulus power and prestimulus EEG activity (-500 – 0 ms) across all frequencies. Subsequently, we subtracted these spontaneous correlations from the Fisher z -transformed desired correlation values for each frequency, thereby isolating the specific correlations of interest. This approach effectively accounted for the baseline or background correlations and allowed us to focus on the target correlations between prestimulus power and poststimulus EEG activity.

To evaluate the impact of prior knowledge on the representational similarity in both standard and deviant trials, we introduced the Influence Index (II), was computed separately for standard and deviant trials using the following equation:

$$II = (\text{rho}_{\text{instr.post}} - \text{rho}_{\text{instr.pre}}) - (\text{rho}_{\text{non-instr.post}} - \text{rho}_{\text{non-instr.pre}}).$$

In this equation, $\text{rho}_{\text{instr.post}}$ represents the averaged correlation values in the instructed condition during the postinstruction session. Similarly, $\text{rho}_{\text{instr.pre}}$ represents the averaged correlation values in the instructed condition during the preinstruction session. Likewise, $\text{rho}_{\text{non-instr.post}}$ represents the averaged correlation values in the noninstructed condition during the postinstruction session, and $\text{rho}_{\text{non-instr.pre}}$ represents the averaged correlation values in the noninstructed condition during the preinstruction session. A positive II value indicates that prior knowledge contributes to an increase in representational similarity, whereas a negative value suggests the opposite.

Decoding analysis. To investigate whether the neural activity for trials in the instructed condition in the postinstruction session carried prior knowledge for different types of stimuli, we built forward models from the EEG signal using the linear discriminant analysis approach (Han et al., 2019; Kok et al., 2017; Shen et al., 2019). We assumed that there is a linear combination of data from different EEG components that can best represent the features of the dog or the face stimuli. Such a neural representation R at time t can be represented as follows:

$$R_t = \alpha_{1,t} \cdot u_{1,t} + \alpha_{2,t} \cdot u_{2,t} + \dots + \alpha_{n,t} \cdot u_{n,t},$$

where $\alpha_{1,t}, \alpha_{2,t}, \dots, \alpha_{n,t}$ are the weights for the linear combination at time t . For the sake of being representative, the neural representation should be similar to each other across different trials for one type of stimulus, but they also should be dissimilar to each other across trials for different types of stimuli. Therefore, to best characterize the face or the

dog stimuli in our experiment, a score function can be created as follows:

$$f(A) = \frac{\text{dist}(R_i^{\text{dog}}, R_i^{\text{face}})}{\text{var}(R_i^{\text{dog}}) + \text{var}(R_i^{\text{face}})},$$

where $A = [\alpha_{1,t}, \alpha_{2,t}, \dots, \alpha_{n,t}]$, $\text{dist}(x, y) = (x - y)^2$ is the function for calculating the Euclidean distance between the neural representation for two types of stimuli, and $\text{var}(\dots)$ is the function to calculate the variance within one type of stimulus. Mathematically, such score function will be maximal when, as follows:

$$A = \frac{\hat{u}_{\text{dog}} - \hat{u}_{\text{face}}}{S_{\text{dog}} + S_{\text{face}}},$$

where $\hat{u} = [\bar{u}_{1,t}, \bar{u}_{2,t}, \dots, \bar{u}_{n,t}]$ is the mean activity over trials for one type of stimulus for all components, and S is the within-stimulus covariance. When such a score function is maximal, the combination weights A are the optimized ones.

In the current analysis, we used all standard trials from the preinstruction and postinstruction sessions in both instructed and noninstructed conditions to obtain the optimal weights for distinguishing between dog and face stimuli. To avoid potential complications caused by an unbalanced number of trials per condition, we matched the number of trials by randomly subsampling the trials in conditions with a larger number of trials (~ 240 standard trials were retained for each condition). To further improve the signal-to-noise ratio, these standard trials were averaged over a 100 ms time window centered on the time point of interest. We trained and tested the classifier using a leave-one-out cross-validation method (Varoquaux et al., 2017). For temporal generalization analysis, the performance of the classifier was evaluated not only at the time point used for training (e.g., classifier $w(t1)$ is tested at $t1$, $w(t2)$ at $t2$, and so on), but also on the data at all other time points (e.g., classifier $w(t1)$ at all time points $t1, t2, t3$, and so on), giving us a (training time) \times (decoding time) temporal generalization matrix (King and Dehaene, 2014). The classifier's performance was evaluated through the utilization of receiver operating characteristic (ROC) curves and the computation of the area under the curve (AUC). This approach yields a sensitive and criterion-free assessment of decoding performance (van Moorselaar et al., 2020).

Statistical analysis. In the GFP analysis, the topographical correlation analysis, and decoding analysis above, the statistical comparison of two conditions was often performed over multiple times or frequency points, which could introduce multiple-comparison problems and inflate the false-positive rate. To control the Type I error rate associated with multiple comparisons, we adopted the nonparametric cluster-based permutation test (Maris and Oostenveld, 2007), which was implemented in a custom script in MATLAB (MathWorks). For the GFP analysis, the topographical correlation analysis, and decoding analyses, the cluster-based correction was applied to compare the difference in GFP, decoding performance, or topographical correlations between different conditions. First, a Student's t test was first performed at the participant level on data from different conditions at each time point, and time points with p values exceeding a prior threshold of 0.05 were marked, and adjacent marked time points were identified as clusters. In the topographical correlation analysis, as we posited a directional hypothesis stating that prestimulus neural representation would exhibit greater similarity to poststimulus neural representation for standard stimuli and less similarity for deviant stimuli when prior knowledge was learned, a one-tailed t test was used. In contrast, for the decoding analysis and GFP analysis, where the objective was to determine whether the decoded information or GFP could differentiate between conditions, regardless of the specific direction, a two-tailed t test was used. The sum of the t values in the cluster was considered as the cluster-level statistic. The data were then shuffled 1000 times between the two conditions. For each shuffle, the maximum cluster statistic was used to construct a distribution of cluster-level statistics, which was expected under the null hypothesis. The p values

were obtained by directly calculating the proportion of cluster statistics that were more extreme than the original data. A p value of 0.001 was assigned when the original data were the most extreme. Finally, cluster-level statistics were considered as significant only if the cluster statistics exceeded the 95th percentile of the null hypothesis distribution (i.e., $\alpha = 0.05$).

To assess the significance of the correlation coefficient between prestimulus alpha power and poststimulus EEG activity, we conducted a permutation test. First, we computed averaged correlation coefficients by averaging the correlations within the alpha band (8–13 Hz) across the entire poststimulus period (50–500 ms) for each participant. Subsequently, a group-level Student's t test was performed against a null hypothesis of zero correlation, and the resulting t statistics were considered as the observed test statistics. Next, we generated 1000 permutations by randomly pairing prestimulus alpha power from one channel with EEG activity from another channel for each participant. For each permutation, we calculated the t statistics using the same method as for the original data, creating a distribution of statistic values under the null hypothesis. To determine the significance, we calculated p values by comparing the observed t statistics with the null distribution. Specifically, a p value of 0.001 was assigned when the observed t statistics were the most extreme. Finally, we considered a statistic value significant only if it exceeded the 95th percentile of the null hypothesis distribution (i.e., $\alpha = 0.05$).

Data availability. All data and code are available at <https://osf.io/xhva5/>. The data and code used in the study are in the public domain for sharing or reuse. The data and code sharing policy adopted by us meets the requirements of the School of Psychology, South China Normal University and has been approved by the institutional ethics committee.

Results

In the present study, similar pictures with and without hidden Dalmatian or human faces were presented as standard and deviant stimuli, respectively, in an oddball paradigm. Prior knowledge about either the dog or the face was introduced in the middle of the experiment. Pictures with prior knowledge were referred to as instructed stimuli and otherwise as noninstructed stimuli. To ensure the perception of the hidden object within the instructed stimuli, participants were allowed to proceed in the experiment only after confidently detecting the presence of the face or dog and accurately identifying the location of its components. After the experiment, participants were asked whether they consciously perceived the hidden objects in the postinstruction session, and all participants confirmed that they were able to perceive them. Participants were asked to perform an irrelevant target detection task (mean hit rate, $97.91\% \pm 1.64$ SD, with all participants achieving a hit rate of $>90\%$), while the target stimuli were independent of the presence or absence of a dog or face feature.

Prior knowledge helps to evoke visual mismatch responses

As the physical properties of the standard and deviant stimuli were similar, it should be difficult to discriminate between them in the absence of prior knowledge, whereas in the presence of prior knowledge, it should be easy to discriminate between them because the face or the dog only appeared in the standard stimuli but not in the deviant stimuli. To verify this, we analyzed the visual mismatch response by calculating the GFP, which not only reflects the overall electrophysiological activity in response to the stimulus but also avoids bias caused by electrode selection. Using the cluster-based method (see above, Materials and Methods), we examined the presence of a visual mismatch response by comparing the standard and deviant stimuli separately for instructed and noninstructed conditions, as well as for preinstruction and postinstruction sessions. In the

preinstruction session, no significant difference in GFP was observed between the instructed and noninstructed conditions (Fig. 2A). This suggests that the physical differences alone between the standard and deviant stimuli did not generate a visual mismatch response in the absence of prior knowledge. In contrast, during the postinstruction session, we identified an early mismatch response specifically in the instructed condition. A significant GFP difference emerged between the deviant and standard conditions within the time interval of 91–142 ms, which was corrected for multiple comparisons using the cluster-based method ($p = 0.021$; Fig. 2B). This finding indicates that after receiving prior knowledge, participants exhibited a robust mismatch response during this early time window, indicating the involvement of prior knowledge in evoking the visual mismatch response. No significant GFP cluster was observed in the postinstruction session for the noninstructed condition, supporting the notion that the visual mismatch response was specific to the instructed stimuli. Furthermore, we examined the topographical distribution of the event-related potential (ERP) difference between the deviant and standard conditions during the time interval of 91–142 ms (Fig. 2C). The results demonstrated that the ERP difference predominantly manifested in the frontal and occipital channels for the instructed stimuli in the postinstruction session.

To determine whether prior knowledge primarily influenced the standard or deviant trials, we analyzed the poststimulus GFP activity within the time interval of 91–142 ms for both standard and deviant trials in instructed and noninstructed conditions, comparing the postinstruction session with the preinstruction session (Fig. 2D). A two (instructed vs noninstructed) by two (standard vs deviant) repeated-measures ANOVA on the difference in GFP signals revealed a significant interaction ($F_{(1,21)} = 5.06$, $p = 0.035$). Further analysis demonstrated no significant difference between instructed and noninstructed conditions for deviant trials ($t_{(21)} = 0.79$, $p = 0.44$). However, significant differences were observed for standard trials ($t_{(21)} = 3.07$, $p = 5.85 \times 10^{-3}$). These findings suggest that prior knowledge primarily has an impact on the poststimulus signal in standard trials, indicating that prior knowledge provides additional information for consciously perceiving the hidden object in the standard stimuli.

Prior knowledge uses prestimulus alpha band oscillations to carry the information about hidden objects

The clear effect of prior knowledge on electrophysiological activity indicates that our psychophysical manipulation was successful. Next, we investigated the neural implementation of prior knowledge before stimulus onset. As prestimulus neural activity often takes the form of neural oscillations, we focused on the relationship between prior knowledge and neural oscillations. The working hypothesis is that if a particular neural oscillation carries the information about the prior knowledge, then the neural representation of such neural oscillations should be similar to the neural representation of the EEG activity during stimulus processing. According to this hypothesis, for the preinstruction session in the instructed condition, because no prior knowledge was provided, the prestimulus neural representation should not be similar to the poststimulus neural representation for both standard and deviant stimuli. Conversely, during the postinstruction session of the instructed condition, the prestimulus neural oscillations are expected to carry information about the prior knowledge of the standard stimuli. This would lead to an increased similarity between the prestimulus neural

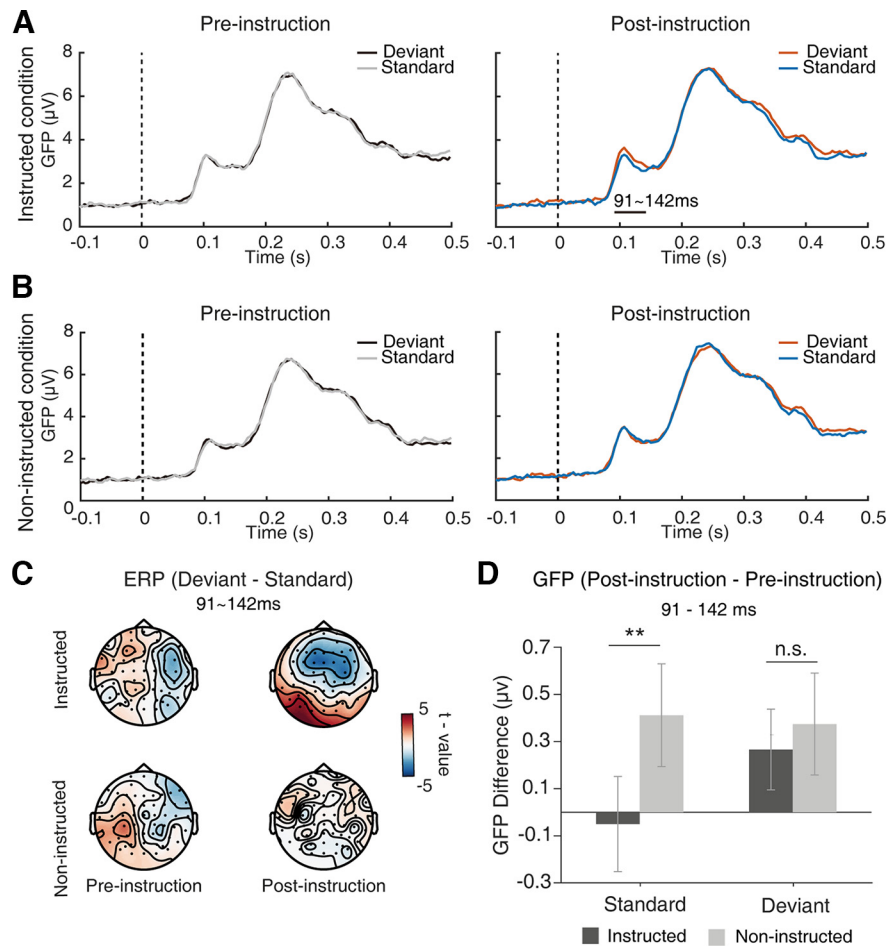


Figure 2. *A*, Comparison of the GFP between the standard and deviant stimuli in the instructed condition for the preinstruction and postinstruction sessions. *B*, Same as *A* but for the noninstructed condition. Significant time points are indicated with horizontal black bars (cluster-based corrected, $p < 0.05$). *C*, Topographic maps illustrating the average event-related potential difference between deviant and standard conditions during the time interval of interest (91–142 ms) for all conditions. *D*, Comparison of GFP differences between postinstruction and preinstruction sessions for standard and deviant trials for instructed and noninstructed stimuli. Error bars represent 95% confidence intervals (Morey, 2008); n.s., $p > 0.05$, ** $p < 0.01$.

representation and the poststimulus neural representation for standard stimuli. In contrast, as the deviant stimuli significantly differ from the prior knowledge, a decreased similarity would be observed for the deviant stimuli (Fig. 3*A*). For the noninstructed condition, there should be no representational similarity effect because no prior knowledge was provided in either the preinstruction or postinstruction sessions.

Specifically, the prestimulus power was first obtained for all channels and frequencies (2–50 Hz) for the time period from –500 to 0 ms relative to the stimulus onset. Accordingly, the poststimulus EEG activity was also obtained for each 100 ms sliding window from 50 to 500 ms after the stimulus onset (see above, Materials and Methods). The representational similarity between the prestimulus power and poststimulus EEG activity was quantified using the correlation coefficient obtained from the topographical correlation analysis (Fig. 3*B*). A higher correlation coefficient indicates a similar topographic representation between prestimulus power and poststimulus EEG activity, whereas a lower correlation coefficient indicates a different topographic representation. Based on our assumptions about prior knowledge, for the instructed condition, we predicted a difference in the correlation coefficients between the standard and deviant stimulus conditions in the postinstruction session, but not in the preinstruction session (Fig. 3*C*). For the noninstructed condition, no difference in correlation coefficients should be observed.

For the instructed stimuli, the results showed that the correlation between prestimulus alpha band oscillatory power and poststimulus EEG activity from ~50 to 390 ms was significantly higher (cluster-based correction, $p = 0.039$) for the standard stimulus condition than for the deviant stimulus condition in the postinstruction session, but not in the preinstruction session (Fig. 4*A*, top). To rule out possible confounding by the practice effect, we performed the same contrast between the preinstruction and postinstruction sessions for the noninstructed stimuli. If the observed representational similarity effect was caused by a practice effect, then a comparable effect should also be observed for the noninstructed stimuli in terms of the difference in correlation coefficients. However, the results showed no such difference for the noninstructed stimuli (Fig. 4*A*, bottom).

To determine whether the representational similarity between prestimulus power and poststimulus EEG activity was indeed higher in the postinstruction session, we conducted a direct comparison of the correlation coefficient differences between the preinstruction and postinstruction sessions. Consistent with our hypothesis, the analysis revealed a significantly larger difference in the postinstruction session compared with the preinstruction session for the instructed stimuli (cluster-based correction, $p = 0.023$; Fig. 4*B*, top). In contrast, no significant differences in correlation coefficient differences were observed for the noninstructed stimuli between the preinstruction and postinstruction

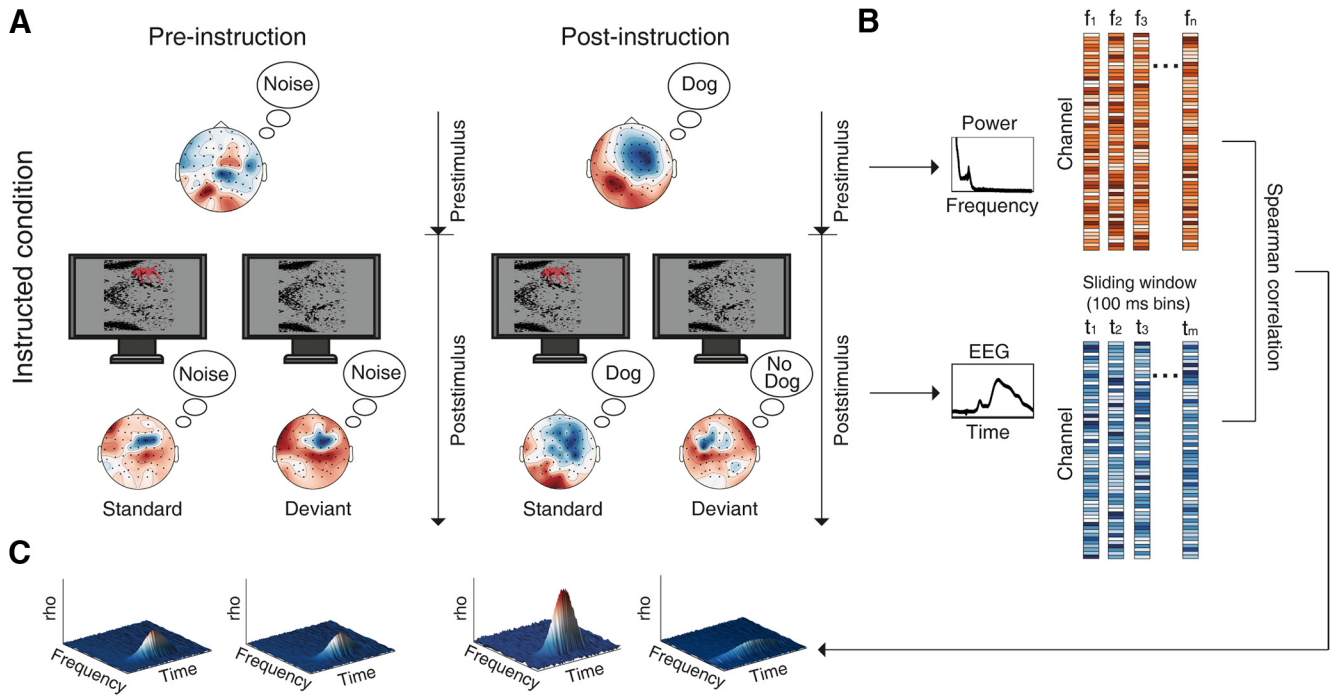


Figure 3. *A*, The hypothesis on the neural representation of prior knowledge during the prestimulus period. For the instructed condition, as no prior knowledge was available in the preinstruction session, the prestimulus neural activity should not be similar to the poststimulus neural activity for both standard and deviant stimuli. However, for the postinstruction session, persistent maintenance of prior knowledge for standard stimuli in the brain during the prestimulus period would lead to an increased similarity between the prestimulus neural representation and the poststimulus neural representation for standard stimuli. In contrast, because of the distinctiveness of the prior knowledge from the deviant stimuli, a decreased similarity would be observed for deviant stimuli. Note that the cue to the hidden object (shown in red) was shown for demonstration purposes only and did not actually appear in the experiment. *B*, A depiction of how the topographical correlation analysis was performed between the prestimulus power and poststimulus EEG activity. Spearman correlations were computed over the channel dimension between prestimulus power at each frequency and poststimulus EEG activity at each time window. *C*, The predicted correlation coefficients for the standard and deviant stimulus conditions in both preinstruction and postinstruction sessions.

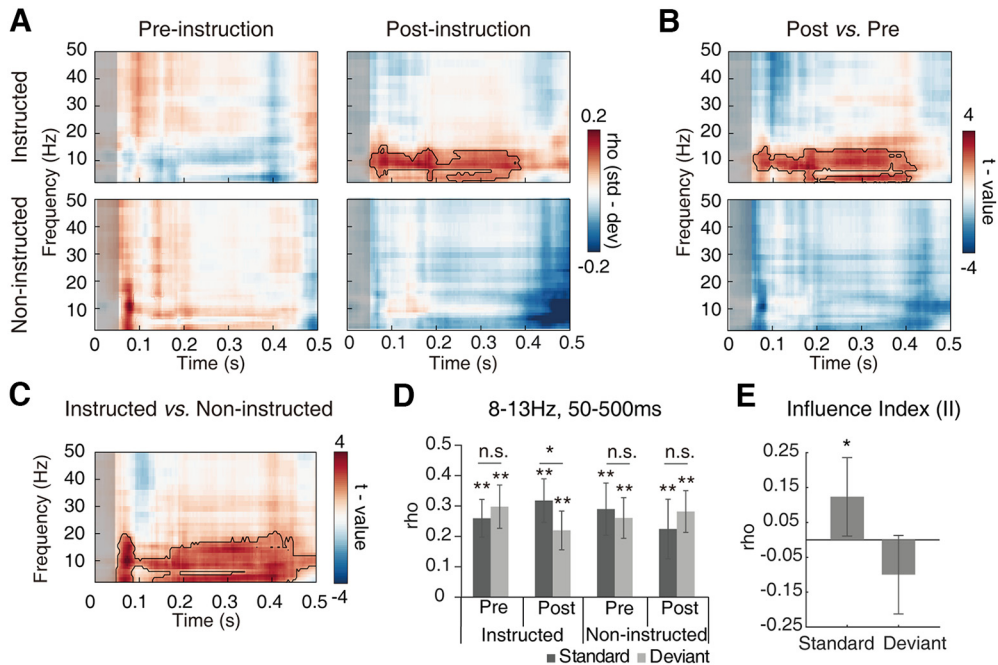


Figure 4. *A*, Differences in correlation coefficients between the standard and deviant stimulus conditions in the preinstruction and postinstruction sessions for the instructed (top) and noninstructed (bottom) stimuli. *B*, Contrasting the differences in correlation coefficients between postinstruction and preinstruction sessions for the instructed (top) and noninstructed (bottom) stimuli. The rows in the plots indicate the time bins of the poststimulus EEG activity, and the columns indicate the frequencies of the prestimulus oscillatory power. Color values indicate the differences in correlation coefficients (*A*) or *t* statistics (*B*, *C*) of the correlation coefficient difference. Significant correlation coefficient differences or contrast of correlation coefficient differences are indicated by the black contours (cluster-based correction, $p < 0.05$). *D*, The average correlation coefficient between the prestimulation alpha band oscillatory power (8–13 Hz) and poststimulation EEG activity (50–500 ms). *E*, II for standard and deviant trials. Error bars represent 95% confidence intervals; n.s., $p > 0.05$, * $p < 0.05$, ** $p < 0.01$.

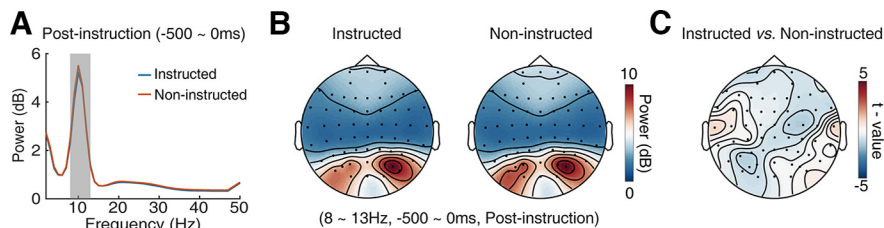


Figure 5. *A*, Comparison of the averaged prestimulus power across all channels for frequencies ranging from 2 to 50 Hz in the postinstruction session. No significant differences were observed for any of the frequencies (all p values > 0.05 , 2-tailed paired t test, uncorrected). *B*, Topographical distribution of prestimulus alpha band power for the instructed and noninstructed conditions in the postinstruction session. *C*, Comparison of the prestimulus alpha band power between the instructed and noninstructed conditions across all channels. No significant differences were found for any of the channels (all p values > 0.05 , 2-tailed paired t test, uncorrected).

sessions (Fig. 4*B*, bottom). Furthermore, we examined the changes in correlation coefficient differences between the postinstruction and preinstruction sessions for both the instructed and noninstructed stimuli, resulting in the subtraction depicted in Figure 4*C*. Notably, the analysis demonstrated that the differences in the alpha band for the instructed stimuli were significantly larger than those for the noninstructed stimuli (cluster-based correction, $p = 0.001$; Fig. 4*C*).

Based on our hypothesis that prestimulus alpha band activity may carry information about prior knowledge, we further conducted statistical analyses on the averaged correlation coefficients (Fig. 4*D*). These coefficients were obtained by averaging the correlations within the alpha band (8–13 Hz) across the entire poststimulus period (50–500 ms). Using a permutation method (see above, Materials and Methods), we first assessed the significance of the correlations. The analysis revealed significant correlations for all conditions (all p values = 0.001), affirming the presence of a relationship between prestimulus alpha power and poststimulus EEG activity. To further investigate the differences in correlations between prestimulus alpha power and poststimulus EEG activity in different conditions, we performed a two (instructed vs noninstructed) by two (preinstruction vs postinstruction) by two (standard vs deviant) ANOVA on the averaged correlation coefficients. Notably, the three-way interaction emerged as the sole significant effect ($F_{(1,21)} = 8.50$, $p = 8.28 \times 10^{-3}$). Further analysis showed a significant two (preinstruction vs postinstruction) by two (standard vs deviant) interaction effect for the instructed condition ($F_{(1,21)} = 5.03$, $p = 0.03$), but not for the noninstructed condition ($F_{(1,21)} = 3.55$, $p = 0.07$). A subsequent simple effect analysis of the instructed condition revealed that the correlation coefficient for the standard stimulus condition was significantly greater than that for the deviant stimulus condition in the postinstruction session ($t_{(21)} = 2.20$, $p = 0.02$), whereas no significant difference was found in the preinstruction session ($t_{(21)} = -1.03$, $p = 0.84$). Consistent with our hypothesis, these findings demonstrated that the neural representation between prestimulus alpha band oscillatory power and poststimulus EEG activity became more similar when prior knowledge was provided, suggesting that alpha band oscillations carry information about prior knowledge during the prestimulus period.

To further evaluate the impact of prior knowledge on the representational similarity in both standard and deviant trials, we calculated the II (see above, Materials and Methods) for standard and deviant trials. The II quantifies the contribution of prior knowledge to changes in representational similarity, with positive values indicating an increase and negative values suggesting a decrease. Our findings revealed a significant positive effect of prior knowledge on representational similarity for standard trials ($t_{(21)} = 2.06$, $p = 0.026$), indicating that prior knowledge

enhances the similarity between prestimulus alpha band oscillatory power and poststimulus EEG activity. Additionally, we observed a trend toward a negative effect of prior knowledge on correlations in deviant trials ($t_{(21)} = -1.67$, $p = 0.054$), suggesting that prior knowledge may lead to a decrease in representational similarity for deviant stimuli (Fig. 4*E*).

To address the potential influence of raw prestimulus alpha band power on the correlation coefficients, we conducted additional analyses. Specifically, we computed the averaged prestimulus power (–500–0 ms) across all channels and frequencies (2–50 Hz) for both the instructed and noninstructed conditions in the postinstruction session. Importantly, no significant differences were observed between the two conditions across all frequencies (all p values > 0.05 ; Fig. 5*A*). Additionally, we specifically examined the prestimulus alpha power (8–13 Hz, –500–0 ms) for all channels in the instructed and noninstructed conditions of the postinstruction session (Fig. 5*B*). Comparisons between the two conditions revealed no significant differences across all channels (all p values > 0.05 ; Fig. 5*C*), suggesting that the observed results were not attributable to variations in alpha band power.

Prior knowledge induces persistent neural templates throughout the poststimulus period

Despite receiving prior knowledge about the hidden Dalmatian dog or face stimuli only once during the instruction, our perceptual experience of these stimuli underwent a significant transformation throughout the postinstruction session. This observation raises intriguing questions about the modulatory effects of prior knowledge on neural activity and the resulting pronounced perceptual effects. It is reasonable to hypothesize that prior knowledge regarding the specific image content has the capacity to induce alterations in the neural representations of these stimuli, surpassing mere differentiation between standard and deviant stimuli. To address this question, we used temporal generalization, a time-resolved decoding method, to examine the differences in neural representations between the face and dog standard stimuli during the preinstruction and postinstruction sessions. In the preinstruction session, the neural representations primarily differed based on physical appearance, with no influence of prior knowledge. However, in the postinstruction session, both physical appearance and prior knowledge contributed to distinct neural representations, as the participants were aware of the stimulus content. Therefore, by comparing the differences in neural representations between the preinstruction and postinstruction sessions, we can uncover the impact of prior knowledge on the brain.

Specifically, the classifiers were first trained for each subject at each time point between the standard face and dog stimuli, using the leave-one-out method for all trials in the preinstruction and

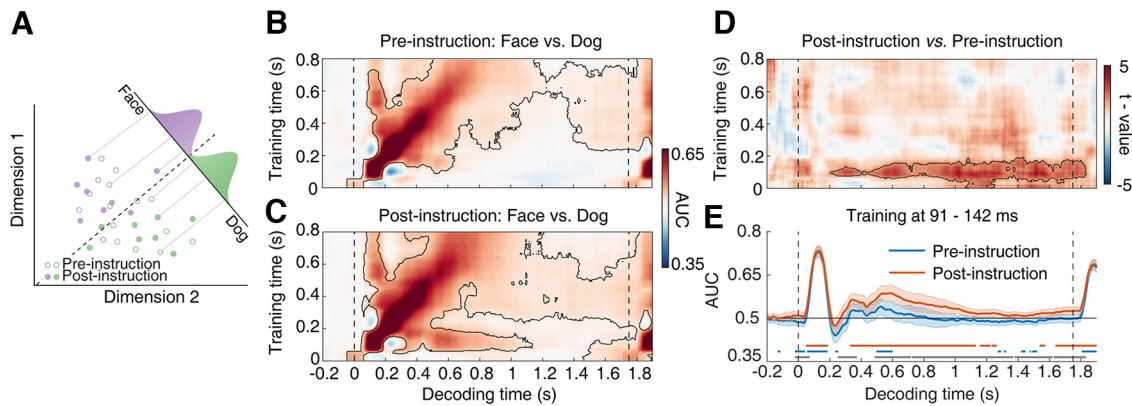


Figure 6. *A*, Hypothetical two-dimensional activation spaces representing the EEG signals of human faces and dogs. Decoding relies on the projection of neural activity in the high-dimensional activation space onto a single-dimensional discriminative axis, regardless of the sessions. Decision boundaries placed along the axes allow for classification between face and dog stimuli. The higher decoding performance indicates a clearer separation of neural representations. *B*, Temporal generalization matrices for the preinstruction session. *C*, Temporal generalization matrices for the postinstruction session. *D*, Temporal generalization matrices for the differential contrast between the preinstruction and postinstruction sessions. Rows in the pictures are the time points at which the classifier was trained, and the columns are the time points at which the classifier was tested. Color values indicate decoding performance in terms of area under the curve (AUC; *B*, *C*) or *t* statistics of AUC difference (*D*). Significant decoding performance is indicated by the black contours (cluster-based correction, $p < 0.05$). *E*, Decoding performance over time when the training time range is set from 91 to 142 ms after stimulus onset. For demonstration purposes, significant generalization time points in the preinstruction session are marked by horizontal red bars, those in the postinstruction session by horizontal blue bars, and the significant difference between them by horizontal gray bars (uncorrected, $p < 0.05$). Shaded areas represent 95% confidence intervals. Dashed lines indicate the stimulus onset.

postinstruction sessions. In this way, the classification relied on the projections of neural activity in the high-dimensional activation space into a single-dimensional space of neural representation, which could maximally separate the neural patterns between the face and dog stimuli regardless of the session (Fig. 6*A*). Then, taking advantage of the temporal generalization method, the classifier trained on one time point was applied on all time points, which allowed direct comparisons of the neural representations between different time points (King and Dehaene, 2014). If the neural representation at a time point is similar to the neural representation at the trained time point, the trained classifier should perform well; on the contrary, if the neural representation is not similar to the neural representation at the trained time point, the trained classifier should perform poorly. The performance of the classifier was quantified by the area under the receiver characteristic curve (see above, Materials and Methods).

We applied the trained classifiers to trials in both the preinstruction and postinstruction sessions. The results showed that the face and dog stimuli could be successfully discriminated for both sessions (Fig. 6*B,C*; cluster-based correction, $p = 0.001$ for the preinstruction session, and $p = 0.001$ for the postinstruction session). More importantly, for the postinstruction session, persistent neural templates were found from ~ 200 ms after the stimulus onset to the end of the trial for classifiers trained on data around 100 ms after the stimulus onset (Fig. 6*D*; cluster-based correction, $p = 0.007$). For demonstration purposes, these generalized signals were further illustrated, for example, when the classifier was trained 91–142 ms after stimulus onset (Fig. 6*E*); the decoding performance of the neural signals from 200 ms after stimulus onset to the end of the trial was better in the postinstruction session compared with the preinstruction session. Please note that in the above GFP analysis, 91–142 ms after stimulus onset is the time window for the visual mismatch response, which is sensitive to the difference between the deviant stimuli (not involved in the current analysis) and the standard stimuli in the postinstruction session. These results suggest that prior knowledge influenced our perception of the hidden Dalmatian dog and face stimuli by generating persistent neural templates

that resemble those evoked during the time window of the visual mismatch response.

To exclude the potential confounds caused by the practice effect, for both preinstruction and postinstruction sessions we divided the trials into two halves according to the order of their occurrence and recalculated the decoding performance. If the observed effects were caused by the practice effect, a gradual change in decoding performance should be observed between the different parts. On the other hand, if the observed effects were caused by the prior knowledge alone, a sudden change in decoding performance should be observed immediately after the instruction. Using the same 91–142 ms window as above, we found little difference in decoding performance between the first and second halves within one session but a substantial difference between the two sessions (Fig. 7*A*). The average decoding performance during the entire poststimulus period also indicated no significant temporal generalization effect in either part during the preinstruction session ($t_{(21)} = 1.52$, $p = 0.14$ for the first half, $t_{(21)} = 1.77$, $p = 0.09$ for the second half; Fig. 7*B*). On the other hand, significant temporal generalization effects were found in both parts during the postinstruction sessions ($t_{(21)} = 3.26$, $p = 3.76 \times 10^{-3}$ for the first half, $t_{(21)} = 4.01$, $p = 6.32 \times 10^{-4}$ for the second half). Then, the average decoding performance was submitted to a two (preinstruction vs postinstruction) by two (first half vs second half) repeated-measures ANOVA. The main effect between the preinstruction and postinstruction was the only significant effect ($F_{(1,21)} = 8.38$, $p = 8.65 \times 10^{-3}$; Fig. 7*B*). Neither the main effect between the first and second half of one session ($F_{(1,21)} = 0.14$, $p = 0.71$), nor the two-way interaction ($F_{(1,21)} = 0.23$, $p = 0.64$), was significant, indicating that effect of practice should not have resulted in the observed effect on decoding performance.

Discussion

In the current study, we investigated the retention of prior knowledge and its effect on conscious perception by revealing the objects hidden inside seemingly meaningless pictures in a visual oddball paradigm (Fig. 1). By comparing the global field

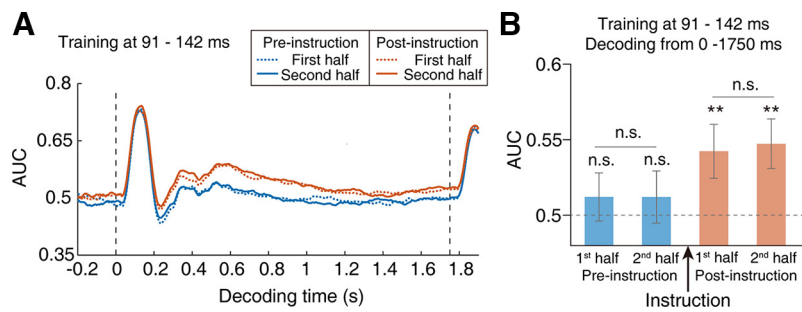


Figure 7. *A*, Decoding performance over time when data from 91 to 142 ms after stimulus onset were used for training. For both preinstruction and postinstruction sessions, the test trials were divided into the two parts (first half and the second half), respectively, according to their order of occurrence. If the observed effects on decoding performance were caused by the practice effect, then a gradual change should be observed between the different parts. *B*, Average decoding performance during the whole poststimulus period (0–1750 ms after stimulus onset) for different parts when the classifiers were trained on data from 91 to 142 ms after stimulus onset. Error bars represent 95% confidence intervals; n.s. $p > 0.05$, ** $p < 0.01$.

power, we found that the visual mismatch response emerged only after the hidden object was revealed, confirming that our psychophysical manipulations to introduce prior knowledge were successful (Fig. 2). To investigate how prior knowledge is maintained during the prestimulus period, we used a multivariate method (Fig. 3) and found that prior knowledge uses alpha band oscillations to convey information about the hidden object (Fig. 4). Furthermore, when we compared neural representations between consciously seen and unseen stimuli, we found that prior knowledge evoked a persistent neural template, similar to the neural representations evoked in the early stages of visual processing, allowing for the conscious perception of hidden objects (Fig. 6).

Accumulating evidence from EEG, magnetoencephalography, and intracranial recordings from animal and human studies consistently suggested that alpha band oscillations are closely associated with the top-down processes in the brain (Klimesch, 2012). However, it remains unclear how the top-down processes use alpha oscillations. On the one hand, a large literature found that top-down processes led to desynchronization of the alpha oscillations. For example, attention reduced alpha activity contralateral to the attended location in both the visual system (Sauseng et al., 2005; Thut et al., 2006; Worden et al., 2000) and the somatosensory system (Haegens et al., 2011). Attention toward one modality also reduced alpha activity in brain regions that process information about that modality (Mazaheri et al., 2014). In addition to attention, temporal expectation has also been shown to reduce alpha activity (Rohenkohl and Nobre, 2011). On the other hand, it has also been reported that top-down modulation can enhance alpha oscillations. For example, in macaque visual cortex, it has been observed that alpha band oscillations propagate in the feedback direction when the animal was able to detect an orientation-defined object in a figure-ground segregation task (van Kerkoerle et al., 2014). Enhanced alpha band oscillations were also found in the visual areas of cats, monkeys, and humans when the stimuli were expected or attended to (Bastos et al., 2020; Chatila et al., 1992; Mayer et al., 2016; J. Mo et al., 2011; Samaha et al., 2018; Stenner et al., 2014). The apparent discrepancy between top-down effects on alpha band oscillations in different studies suggests that the top-down control can both enhance and attenuate the alpha band oscillations in different brain regions at the same time, depending on their location and function (Sauseng et al., 2005; Worden et al., 2000). In the current study, rather than an overall univariate enhancement or attenuation of alpha band oscillations, the results show that prior knowledge uses prestimulus alpha band oscillations in a multivariate manner; that is, there is a similar topographic pattern between prestimulus alpha band oscillations and poststimulus

EEG activity. Together with recent studies on the neural representation of alpha band oscillations (Samaha et al., 2016; Voytek et al., 2017; de Vries et al., 2021), the current results provide insight into the role of prestimulus alpha oscillations from a multivariate perspective. However, because of the experimental design limitations of our study, which only revealed either the hidden dog or the hidden face but not both, we were unable to directly examine whether and how the prestimulus alpha power carrying prior knowledge of the dog differs from the prestimulus alpha power carrying prior knowledge of the face. This intriguing question could serve as a research topic for future investigations.

Once acquired, prior knowledge alters our perception and produces a persistent conscious perception, so it is conceivable that the neural representation of such experience persists in ongoing brain states. Several studies have provided evidence for this possibility. For example, by comparing the consciously seen and unseen stimuli, previous studies have reported that conscious perception is associated with a sustained neural activity in different brain areas (Li et al., 2014), resulting in a stronger neural representation of the stimuli (King et al., 2016; Salti et al., 2015). In the current study, however, instead of a stronger neural representation, we found persistent neural templates that resemble the neural representations evoked in the early stages of visual processing. One possible explanation for the different results is that previous studies relied on subjects' responses to determine whether the stimuli were consciously perceived, which involves neural correlates for both conscious experience and postconscious processes (Aru et al., 2012), whereas in the current study, because conscious perception was task irrelevant, the persistent neural templates may reflect neural correlates for conscious experience only. In addition, very similar persistent neural templates were found in an MEG study of object recognition, and it was suggested that such persistent neural representations may store the results of a particular neural processing stage for later use (Cichy et al., 2014). It is possible that these persistent neural templates maintain the conscious perception of the hidden objects for further processing when needed, similar to recent findings that prior expectations induce neural templates to improve corresponding behavioral performance (Kok et al., 2017).

As attention to the location of the corresponding hidden object may be enhanced because of the acquisition of specific prior knowledge, one can assume that attention (which has been extensively studied) gives rise to the observed effects between preinstruction and postinstruction sessions or between standard and deviant stimuli. However, in the current study, our experimental design and results suggest that this is highly

unlikely. For the experimental design, to minimize the effects of attention, we used a task-independent oddball paradigm in a fast-learning experiment. In such a paradigm, because the stimuli in the preinstruction and postinstruction sessions or in the standard and deviant conditions were exactly or nearly identical, it is unlikely the observed effects were influenced by the bottom-up attention. Moreover, revealing hidden objects between the preinstruction and postinstruction sessions could not improve the performance on the experimental task; that is, it is task irrelevant, and the sequence of standard and deviant stimuli was randomized. Therefore, top-down attention should be similar across different conditions, at least in the prestimulus period. In terms of the experimental results, effects induced by prior knowledge appeared fairly early in the poststimulus period; for example, the observed differences in representational similarity began ~50 ms after stimulus onset, and the observed persistent multivariate patterns resemble neural representation from 91 to 142 ms after stimulus onset as the effect of attention is expected to manifest later (e.g., N2pc, P300), it is unlikely that prior knowledge affects the brain through post-stimulus attentional mechanisms. Together, because the experimental design ensured that the prestimulus attention was similar across different conditions, and the observed effects were too early for poststimulus attentional mechanisms, the observed effect should directly reflect the influence of prior knowledge rather than the modulation of attention.

In summary, the present study aimed to investigate how prior knowledge influences conscious perception. Our findings provided direct evidence that prior knowledge uses prestimulus alpha oscillations to carry the information about the hidden objects in a multivariate manner. Furthermore, prior knowledge persistently influences conscious perception in the poststimulus period by inducing specific neural representations that resemble the early stages of visual processing, which may be a key factor in conscious perception.

References

- Ahissar M, Hochstein S (2004) The reverse hierarchy theory of visual perceptual learning. *Trends Cogn Sci* 8:457–464.
- Albright TD (2012) On the perception of probable things: neural substrates of associative memory, imagery, and perception. *Neuron* 74:227–245.
- Aru J, Bachmann T, Singer W, Melloni L (2012) Distilling the neural correlates of consciousness. *Neurosci Biobehav Rev* 36:737–746.
- Bar M (2004) Visual objects in context. *Nat Rev Neurosci* 5:617–629.
- Bastos AM, Lundqvist M, Waite AS, Kopell N, Miller EK (2020) Layer and rhythm specificity for predictive routing. *Proc Natl Acad Sci U S A* 117:31459–31469.
- Brainard DH (1997) The psychophysics toolbox. *Spatial Vis* 10:433–436.
- Chang R, Baria AT, Flounders MW, He BJ (2016) Unconsciously elicited perceptual prior. *Neurosci Conscious* 2016:niw008.
- Chatila M, Milleret C, Buser P, Rougeul A (1992) A 10 Hz “alpha-like” rhythm in the visual cortex of the waking cat. *Electroencephalogr Clin Neurophysiol* 83:217–222.
- Cichy RM, Pantazis D, Oliva A (2014) Resolving human object recognition in space and time. *Nat Neurosci* 17:455–462.
- Dehaene S (2014) *Consciousness and the brain: deciphering how the brain codes our thoughts*. New York: Penguin.
- de Lange FP, Heilbron M, Kok P (2018) How do expectations shape perception? *Trends Cogn Sci* 22:764–779.
- de Vries IEJ, Marinato G, Baldauf D (2021) Decoding object-based auditory attention from source-reconstructed MEG alpha oscillations. *J Neurosci* 41:8603–8617.
- Gregory RL (1970) *The intelligent eye*. New York: McGraw-Hill.
- Haegens S, Händel BF, Jensen O (2011) Top-down controlled alpha band activity in somatosensory areas determines behavioral performance in a discrimination task. *J Neurosci* 31:5197–5204.
- Han B, Mostert P, de Lange FP (2019) Predictable tones elicit stimulus-specific suppression of evoked activity in auditory cortex. *Neuroimage* 200:242–249.
- Han B, Zhang Y, Shen L, Mo L, Chen Q (2023) Task demands modulate prestimulus alpha frequency and sensory template during bistable apparent motion perception. *Cereb Cortex* 33:1679–1692.
- Helmholtz H. v (1867) *Handbuch der physiologischen Optik: mit 213 in den Text eingedruckten Holzschnitten und 11 Tafeln*. Leipzig, Germany: Voss.
- King J-R, Dehaene S (2014) Characterizing the dynamics of mental representations: the temporal generalization method. *Trends Cogn Sci* 18:203–210.
- King J-R, Pescetelli N, Dehaene S (2016) Brain mechanisms underlying the brief maintenance of seen and unseen sensory information. *Neuron* 92:1122–1134.
- Klimesch W (2012) α -band oscillations, attention, and controlled access to stored information. *Trends Cogn Sci* 16:606–617.
- Kok P, Mostert P, de Lange FP (2017) Prior expectations induce prestimulus sensory templates. *Proc Natl Acad Sci U S A* 114:10473–10478.
- Li Q, Hill Z, He BJ (2014) Spatiotemporal dissociation of brain activity underlying subjective awareness, objective performance and confidence. *J Neurosci* 34:4382–4395.
- Lehmann D, Skrandies W (1980) Reference-free identification of components of checkerboard-evoked multichannel potential fields. *Electroencephalogr Clin Neurophysiol* 48:609–621.
- Maris E, Oostenveld R (2007) Nonparametric statistical testing of EEG- and MEG-data. *J Neurosci Methods* 164:177–190.
- Mayer A, Schwiedrzik CM, Wibrall M, Singer W, Melloni L (2016) Expecting to see a letter: alpha oscillations as carriers of top-down sensory predictions. *Cereb Cortex* 26:3146–3160.
- Mazaheri A, van Schouwenburg MR, Dimitrijevic A, Denys D, Cools R, Jensen O (2014) Region-specific modulations in oscillatory alpha activity serve to facilitate processing in the visual and auditory modalities. *Neuroimage* 87:356–362.
- Mo J, Schroeder CE, Ding M (2011) Attentional modulation of alpha oscillations in macaque inferotemporal cortex. *J Neurosci* 31:878–882.
- Mo L, Xu G, Kay P, Tan L-H (2011) Electrophysiological evidence for the left-lateralized effect of language on preattentive categorical perception of color. *Proc Natl Acad Sci U S A* 108:14026–14030.
- Morey RD (2008) Confidence intervals from normalized data: a correction to Cousineau (2005). *TQMP* 4:61–64.
- Oostenveld R, Fries P, Maris E, Schoffelen J-M (2011) FieldTrip: Open source software for advanced analysis of MEG, EEG, and invasive electrophysiological data. *Comput Intell Neurosci* 2011:156869.
- Rohenkohl G, Nobre AC (2011) α oscillations related to anticipatory attention follow temporal expectations. *J Neurosci* 31:14076–14084.
- Sadil P, Potter KW, Huber DE, Cowell RA (2019) Connecting the dots without top-down knowledge: evidence for rapidly-learned low-level associations that are independent of object identity. *J Exp Psychol Gen* 148:1058–1070.
- Salti M, Monto S, Charles L, King J-R, Parkkonen L, Dehaene S (2015) Distinct cortical codes and temporal dynamics for conscious and unconscious percepts. *Elife* 4:e05652.
- Samaha J, Bauer P, Cimaroli S, Postle BR (2015) Top-down control of the phase of alpha-band oscillations as a mechanism for temporal prediction. *Proc Natl Acad Sci U S A* 112:8439–8444.
- Samaha J, Sprague TC, Postle BR (2016) Decoding and reconstructing the focus of spatial attention from the topography of alpha-band oscillations. *J Cogn Neurosci* 28:1090–1097.
- Samaha J, Boutonnet B, Postle BR, Lupyan G (2018) Effects of meaningfulness on perception: alpha-band oscillations carry perceptual expectations and influence early visual responses. *Sci Rep* 8:6606.
- Sauseng P, Klimesch W, Stadler W, Schabus M, Doppelmayr M, Hanslmayr S, Gruber WR, Birbaumer N (2005) A shift of visual spatial attention is selectively associated with human EEG alpha activity. *Eur J Neurosci* 22:2917–2926.
- Schurger A, Sarigiannidis I, Naccache L, Sitt JD, Dehaene S (2015) Cortical activity is more stable when sensory stimuli are consciously perceived. *Proc Natl Acad Sci U S A* 112:E2083–E2092.
- Shen L, Han B, Chen L, Chen Q (2019) Perceptual inference employs intrinsic alpha frequency to resolve perceptual ambiguity. *PLoS Biol* 17:e3000025.

- Stenner M-P, Bauer M, Haggard P, Heinze H-J, Dolan R (2014) Enhanced alpha-oscillations in visual cortex during anticipation of self-generated visual stimulation. *J Cogn Neurosci* 26:2540–2551.
- Thut G, Nietzel A, Brandt SA, Pascual-Leone A (2006) Alpha-band electroencephalographic activity over occipital cortex indexes visuospatial attention bias and predicts visual target detection. *J Neurosci* 26:9494–9502.
- van Kerkoerle T, Self MW, Dagnino B, Gariel-Mathis M-A, Poort J, van der Togt C, Roelfsema PR (2014) Alpha and gamma oscillations characterize feedback and feedforward processing in monkey visual cortex. *Proc Natl Acad Sci U S A* 111:14332–14341.
- van Tonder GJ, Ejima Y (2000) Bottom-up clues in target finding: why a Dalmatian may be mistaken for an elephant. *Perception* 29:149–157.
- Varoquaux G, Raamana PR, Engemann DA, Hoyos-Idrobo A, Schwartz Y, Thirion B (2017) Assessing and tuning brain decoders: cross-validation, caveats, and guidelines. *Neuroimage* 145:166–179.
- von Stein A, Chiang C, König P (2000) Top-down processing mediated by interareal synchronization. *Proc Natl Acad Sci U S A* 97:14748–14753.
- Voytek B, Samaha J, Rolle CE, Greenberg Z, Gill N, Porat S, Kader T, Rahman S, Malzyner R, Gazzaley A (2017) Preparatory encoding of the fine scale of human spatial attention. *J Cogn Neurosci* 29:1302–1310.
- Wilsch A, Henry MJ, Herrmann B, Maess B, Obleser J (2015) Alpha oscillatory dynamics index temporal expectation benefits in working memory. *Cereb Cortex* 25:1938–1946.
- Worden MS, Foxe JJ, Wang N, Simpson GV (2000) Anticipatory biasing of visuospatial attention indexed by retinotopically specific alpha-band electroencephalography increases over occipital cortex. *J Neurosci* 20:RC63–RC63.
- Wutz A, Melcher D, Samaha J (2018) Frequency modulation of neural oscillations according to visual task demands. *Proc Natl Acad Sci U S A* 115:1346–1351.
- van Moorselaar D, Lampers E, Cordesius E, Slagter HA (2020) Neural mechanisms underlying expectation-dependent inhibition of distracting information. *eLife* 9:e61048.